Notes on the modeling of Kerr black holes: QNM frequencies, separation constants, and spherical-spheroidal mixing coefficients

L. T. London[1]

[1]*School of Physics and Astronomy, Cardiff University, The Parade, Cardiff, CF24 3AA, United Kingdom*

(Dated: May 24, 2018)

Here I summarize the structure of a multi-mode ringdown model for implementation in the LIGO Analysis Library. The model of discussion has been tuned to binary black hole systems with initial non-spinning progenitors. The current model, as well as its more general progeny may be used to directly compare the post-merger radiation of detected binary black hole systems to the predictions of classical black hole perturbation theory. For sufficiently, high SNR signals, this comparison enables testing of the No-Hair Theorem, which in turn would confer an new experimental test of how well Einstein's general relativity describes these systems.

a. Introduction:— The authors of [1] have presented a rudimentary model for the Quasi-Normal Mode (QNM) excitations resulting from initially nonspinning black hole binary mergers: QNM amplitudes and physical intrinsic phases were modeled for leading fundamental QNMs and overtones. At the time of its publication, this was arguably the most advanced model for astrophysically relevant black hole QNMs. Here, we build directly upon these results by presenting a simplified formulation of the model that is tailored for the LIGO Analysis Library (LAL). The presented reformulation conforms to LAL conventions and standards, thereby supporting the following scientific objectives: true multi-mode parameter estimation for ringdown signals (where physical relationships between the modes are enforced), tests of the No Hair Theorem for gravitational wave signals whose progenitor is consistent with initially nonspinning black hole binaries, and a reference for future QNM analysis upon systems with general progenitors.

While the observable gravitational wave signal has polarizations, h_+ and $h_\times$, which correspond to a detector response[1],

$$h^{\text{Resp.}}(t) \;=\; h_+(t)\,F_+ \,+\, h_\times(t)\,F_\times \;,$$

from the perspective of Numerical Relativity, it is most convenient to consider

$$\psi_4 = \frac{d^2}{dt^2}\,h = \frac{d^2}{dt^2}\;(\,h_+ - i\,h_\times\,)\,. \tag{1}$$

In the case of binary black holes, once the two objects have merged, the *ringing down* radiation from the distorted remnant black hole may be written[2] in the time domain as

$$\psi_4(t,r,\theta,\phi) = \frac{1}{r}\sum_{k\,\leftrightarrow\,\{l,m,n\}} A_k\,S_k(\theta,\phi)\,\exp\left(i\tilde{\omega}_k t\right)\,, \tag{2}$$

where θ and ϕ define polar and azimuthal angles in the source frame, r is the distance from the observer to the source, and $S_k(\theta,\phi)$ are the spin -2 weighted *Spheriodal Harmonic* functions. Note that we have chosen a simplified label, k, for each spheroidal harmonic multipole term. The label k may be thought of as a bijective encoding of the polar and azimuthal indices, l and m, as well as the "overtone" number, n. Here, we will label QNMs by k when specific (l,m,n) are not needed explicitly. In Equation (2), A_k is the complex amplitude of multipolar term, meaning

$$A_k \;=\; |A_k|\,e^{i\,\phi_k}\;. \tag{3}$$

It is of particular utility to note that $S_k(\theta,\phi)$, unlike their spherical harmonic counterparts, ${}_{-2}Y_{lm}(\theta,\phi)$, are not orthonormal. Semantically, this means that the multipolar terms in Equation (2) are not normal modes of the physical system, but rather QNMs.

Given the remnant black hole's mass, M_f, and spin $|\vec{S}_f|$, black hole perturbation theory predicts the *dimensionless* and complex valued QNM frequencies,

$$\begin{aligned}\tilde{\Omega}_k \;&=\; M_f\tilde{\omega}_k \;=\; M_f(\omega_k \,+\, i/\tau_k) \\ &=\; \Omega^{\text{r}}_k \,+\, i\Omega^{\text{c}}_k\end{aligned} \tag{4}$$

However, as the QNM frequencies are directly related to the eigenvalue problem of the perturbed Kerr spacetime, full Numerical Relativity is needed to determine the QNM amplitudes, A_k.

In particular, given the initial binary mass-ratio and spins, $\boldsymbol{\lambda} = \{\eta, \vec{S}_1, \vec{S}_2\}$, where η is related to the bninary's component masses via

$$\eta = m_1 m_2/(m_1+m_2)^2\;,$$

it is reasonable to expect that, for quasi-circular inspirals, these parameters constrain the system's initial[3] conditions such that the QNM excitations of the remnant black hole may be thought of as $A_k \;=\; A_k(\boldsymbol{\lambda})$. Therefore, a set of N Numerical Relativity simulations labeled by $\{\boldsymbol{\lambda}_u\}_{u=1}^N$ enables the construction of a continuous map $A_k : \{\boldsymbol{\lambda}\} \mapsto A_k(\boldsymbol{\lambda})$ through an interpolation over $\{\boldsymbol{\lambda}_u\}_{u=1}^N$. In this sense, a model for the gravitational radiation of ringdown depends on a model for the QNM excitation amplitudes on the space of initial binary parameters.

The model presented here, which is encapsulated by Equations (5-13), builds upon the work of [1] and is applicable to ~~initially nonspinning~~ non-precessing binary black hole systems. Compared to [1], the model presented here has a simpler functional dependence, and most importantly, the current model has been implemented in LAL under the waveform approximant name `MMRDNS`.

[1] See *e.g.* [2] for details on F_+ and $F_\times$.

[2] This is an empirical approximation supported by direct numerical evaluation of full General Relativity.

[3] Here initial means the unbounded regime of very early inspiral, where the system is accurately described by Post-Newtonian theory.

$$A_{220}(\eta) = \omega^2_{220}\,(\,0.9585\,e^{2.9932i}\eta + 0.4759\,e^{0.8266i}\eta^2 + 1.2385\,e^{2.3053i}\eta^3\,) \quad (5)$$

$$A_{221}(\eta) = \omega^2_{221}\,(\,0.1275\,e^{0.0581i}\eta + 1.1882\,e^{1.5180i}\eta^2 + 8.2709\,e^{4.4201i}\eta^3 + 26.2329\,e^{1.1678i}\eta^4\,) \quad (6)$$

$$A_{210}(\eta) = \omega^2_{210}\,\sqrt{1-4\eta}\,(\,0.4795\,e^{5.9656i}\eta + 1.1736\,e^{3.9747i}\eta^2 + 1.2303\,e^{2.1732i}\eta^3\,) \quad (7)$$

$$A_{330}(\eta) = \omega^2_{330}\,\sqrt{1-4\eta}\,(\,0.4247\,e^{4.5473i}\eta + 1.4742\,e^{2.7019i}\eta^2 + 4.3139\,e^{5.1282i}\eta^3 + 15.7264\,e^{2.2547i}\eta^4\,) \quad (8)$$

$$A_{331}(\eta) = \omega^2_{331}\,\sqrt{1-4\eta}\,(\,0.1480\,e^{2.0396i}\eta + 1.4874\,e^{5.8954i}\eta^2 + 10.1637\,e^{3.2835i}\eta^3 + 29.4786\,e^{0.8106i}\eta^4\,) \quad (9)$$

$$A_{320}(\eta) = \omega^2_{320}\,(\,0.1957\,e^{0.5433i}\eta + 1.5830\,e^{4.2451i}\eta^2 + 5.0338\,e^{1.7100i}\eta^3 + 3.7366\,e^{5.1474i}\eta^4\,) \quad (10)$$

$$A_{440}(\eta) = \omega^2_{440}\,(\,0.2531\,e^{5.1632i}\eta + 2.4040\,e^{2.4690i}\eta^2 + 14.7273\,e^{5.5624i}\eta^3 + 67.3624\,e^{2.1982i}\eta^4 + 126.5858\,e^{5.4174i}\eta^5\,) \quad (11)$$

$$A_{430}(\eta) = \omega^2_{430}\,\sqrt{1-4\eta}\,(\,0.0938\,e^{2.3077i}\eta + 0.8273\,e^{6.1005i}\eta^2 + 3.3385\,e^{3.8733i}\eta^3 + 4.6639\,e^{1.7517i}\eta^4\,) \quad (12)$$

$$A_{550}(\eta) = \omega^2_{550}\,\sqrt{1-4\eta}\,(\,0.1548\,e^{1.0675i}\eta + 1.5091\,e^{4.5498i}\eta^2 + 8.9333\,e^{1.2898i}\eta^3 + 42.3431\,e^{4.1004i}\eta^4 + 89.1947\,e^{1.0251i}\eta^5\,) \quad (13)$$

b. Methods – A key technical point must be confronted in order to model the QNM amplitudes, $A_k(\eta)$: Numerical Relativity represents ψ_4 according to spherical multipoles

$$\psi_4(t,r,\theta,\phi) = \frac{1}{r}\sum_{l',m'} \psi_{l'm'}(t)\;{}_{-2}Y_{l'm'}(\theta,\phi) \quad (14)$$

where

$$\psi_{l'm'}(t) = \int_\Omega {}_{-2}\bar{Y}_{l'm'}(\theta,\phi)\, r\psi_4(t,r,\theta,\phi)\;\mathrm{d}\Omega \quad (15)$$

while the perspective of black hole perturbation theory (i.e. solutions to Teukolsy's master equations) correspond to Equation (2). The practical consequence is that, during ringdown, Numerical Relativity's spherical harmonic multipoles, $\psi_{l'm'}$, correspond to a sum of QNM terms[4]. This can be shown by substituting $r\psi_4$ from Equation (2) into Equation (15)'s right hand side, yielding

$$\psi_{l'm'}(t) = \sum_k A_k\,\sigma_{l'm'k}\,\exp(i\,\tilde{\omega}_k\,t) \quad (16)$$

where

$$\sigma_{l'm'k} = \int_\Omega {}_{-2}\bar{Y}_{l'm'}(\theta,\phi)\,S_k(\theta,\phi)\;\mathrm{d}\Omega\,. \quad (17)$$

As the $\psi_{l'm'}$ are the primary data product of Numerical Relativity simulations, constructing $A_k(\boldsymbol{\lambda})$ requires the self-consistent extraction of each A_k from Equation (16). Note that as $S_k \propto e^{im\phi}$ and ${}_{-2}\bar{Y}_{l'm'} \propto e^{im'\phi}$, it follows that $\sigma_{l'm'k} = \sigma_{l'm'lmn} \propto \delta_{m'm}$. Therefore, within a given Numerical Relativity multipole $\psi_{l'm'}$, only QNMs of $m = m'$ will appear. This significantly simplifies the extraction of each A_k.

In particular, this orthogonality in m enables Equation (16) to be framed as a set of normal equations in the least squares sense. This may be quickly illustrated by considering Equation (16)'s abstract vector analog

$$|\psi_j\rangle = \sum_k B_{jk}\,|z_k\rangle, \text{ where } j \leftrightarrow (l'm'), \text{ and } B_{jk} = A_k\,\sigma_{jk}\,. \quad (18)$$

[4] This statement is particular to the systems considered here, and is known to not generally be true CITE.

In this notation, the frequency domain projection of $|z_k\rangle$ at the p^{th} QNM central frequency is

$$\langle\omega_p|z_k\rangle = \int_{t_0}^{t_1} \exp(-i\omega_p t)\;\exp(i\tilde{\omega}_k t)\;\mathrm{d}t \quad (19)$$

where $[t_0, t_1]$ is a chosen region within Numerical Relativity's $\psi_{l'm}$ where QNMs are expected to dominate. In the same way, we may define $\langle\omega_p|\psi_j\rangle$. Thus, acting on both sides of Equation (18) with $\langle\omega_p|$ gives

$$\langle\omega_p|\psi_j\rangle = \sum_k B_{jk}\,\langle\omega_p|z_k\rangle\,. \quad (20)$$

Note that, like k, $p \leftrightarrow (l,m,n)$. Furthermore, it is useful to note that j plays no algebraically significant role in Equation (20). This means that we may read Equation (20) as: *a vector with elements labeled by p* is equivalent to *a matrix in p and k operating on another vector in k*. Specifically, if we associate the p^{th} element of a vector $\vec{\alpha}$ with $\langle\omega_p|\psi_j\rangle$, the k^{th} element of a vector $\vec{\beta}$ with B_{jk}, and the (p,k) elements of a matrix $\hat{Q}$ with $\langle\omega_p|z_k\rangle$, then Equation (20) takes the form

$$\vec{\alpha} = \hat{Q}\vec{\beta}, \text{ or equivalently, } \alpha_p = Q^k{}_p\,\beta_k\,. \quad (21)$$

The utility of Equation (21) is that it allows us to easily solve for $A_k\sigma_{jk}$ via

$$\vec{\beta} = \hat{Q}^{-1}\,\vec{\alpha} \quad (22)$$

Pursuant to transparency, we recall that $A_k\sigma_{jk}$ *are* elements of the vector $\vec{\beta}$, where k is the distinguishing label.

One should in principle be concerned about the well-posedness of the system of equations given by Equation (21). For example, if for some $p \neq p'$, we have that $\langle\omega_p|z_k\rangle \propto \langle\omega_{p'}|z_k\rangle\;\forall\,k$, then $\hat{Q}$ will be singular. This should be of moderate concern for highly spinning black holes (*i.e.* $j_f = |\vec{S}_f|/M_f^2 \sim 1$), where the frequencies of different overtones become very similar. Independently, this should be of concern for more than linear order perturbations of the background spacetime, which more densely populate the space of possible QNM frequencies. However, for the cases of current interest, linear order perturbations, where $j_f \sim 0.7$, we find that $\hat{Q}$ is *always* non-singular within the accuracy allowed by current Numerical Relativity.

Bringing all of these ideas together, we have that the multipoles of Numerical Relativity, $\psi_{l'm'}$, are sums of QNMs during ringdown, and that each QNM's complex amplitude can be extracted according to

$$A_k \;=\; \{\hat{Q}^{-1}\,\vec{\alpha}\}_k \;/\; \sigma_{jk}\;. \tag{23}$$

In seeking to construct a map between A_k and the continuous space of initial binary parameters $\boldsymbol{\lambda}$, Equation (23) should be considered for each simulation of interest, and then interpolated. However, a number of additional technical obstacles remain to be identified and managed. Most prominently, a number of careful steps must be taken to process the complex QNM amplitudes from Equation (23) for modeling.

c. The construction of $A_k(\boldsymbol{\lambda})$:— We seek to construct a map between the space of initial binary parameters, $\boldsymbol{\lambda}$, and QNM excitation amplitudes A_k. We wish this map to accurately represent the results of applying Equation (23) to Numerical Relativity data; therefore, the map must be *trained to* a set of N Numerical Relativity simulations with initial parameters $\{\boldsymbol{\lambda}_u\}_{u=1}^{N}$. However, it must be considered that each estimate of A_k resulting from Equation (23) will, upon evaluation, contain *extrinsic* properties resulting from arbitrary simulation choices that are not intrinsic to the initial conditions $\boldsymbol{\lambda}_u$.

Principally, upon noting that A_k is a complex number with amplitude $|A_k|$ and phase ϕ_k (Equation 3), each ϕ_k has an intrinsic and extrinsic contributions

$$\phi_k \;=\; \phi_k^{\text{Extrensic}} + \varphi_k \tag{24}$$

The most prevalent of these extrinsic properties results from the definition of the fitting region defined in Equation (19). Specifically, t_1 affects the magnitude and phase of each A_k according to:

$$A_k(t') \;=\; A_k(t_1)\,\exp(i\,\tilde{\omega}_k\,[t'-t_1]) \tag{25}$$

I. LIVE NOTES

a. On the nearly extremally damped QNMs: — Here, the $(l,m,n)\in\{(2,1,0),(3,2,0)\}$ QNMs have been numerically found to be damped modes in the nearly extremal Kerr regime. We find that their fitting formula require a higher polynomial degree in order to achieve residual error comparable to their zero-damped mode counterparts.

b. How many QNM for a single spin value, l, m and n?: — Here we attempt to clarify how many QNM solutions there are for a given (j_f,l,m,n). There are two. This in conjunction with conjugate symmetry (*i.e.* $m\to -m$), means that there are actually four. Got it??

c. QNM Labeling Convention: — Note that we use a labeling convention for the QNMs such that

Prograde	$j_f \geq 0$	$\text{sign}(\text{re}(\omega_{lmn})) = \text{sign}(m)$
Retrograde	$j_f < 0$	$\text{sign}(\text{re}(\omega_{lmn})) = \text{sign}(m)$

and the full wave solution is of the form

$$\begin{aligned} r\psi_k = &\sum_{k,\,j_f\geq 0} A_k\, e^{i\tilde{\omega}_k t} S_k(j_f\tilde{\Omega}_k,\theta,\phi) \\ &+ \sum_{k,\,j_f<0} \left(A_k\, e^{i\tilde{\omega}_k t}\right)^* S_k(j_f\tilde{\Omega}_k^*,\theta,\phi)\;. \end{aligned} \tag{26}$$

This differs from the convention used in [3], which holds that j_f is always positive and

Prograde	$j_f \geq 0$	$\text{sign}(\text{re}(\omega_{lmn})) = \text{sign}(m)$
Retrograde	$j_f \geq 0$	$\text{sign}(\text{re}(\omega_{lmn})) = -\text{sign}(m)$

making the full *real-valued* waveform solution

$$\begin{aligned} r\psi_k = &\sum_{k} A_k\, e^{i\tilde{\Omega}_k t} S_k(j_f\tilde{\Omega}_k,\theta,\phi) \\ &+ \sum_{k} \left(A_k\, e^{i\tilde{\Omega}_k t}\right)^* S_k(j_f\tilde{\Omega}_k^*,\theta,\phi)\;. \end{aligned} \tag{27}$$

Note that both conventions differ by a trivial relabeling of terms and result in the same *real-valued* waveform.

d. Symmetry Relationships: — Note that the following symmetry relationships apply to the QNM frequencies, $\tilde{\omega}_{lmn}$ and their related separation constants, $\mathcal{K}_{lmn}$:

$$\tilde{\omega}_{l-mn} = -\tilde{\omega}^*_{lmn}\,, \quad \mathcal{K}_{l-mn} = \mathcal{K}^*_{lmn} \tag{28}$$

e. Different Perturbations: — In some extreme mass ratio cases, it appears that the frequency of the time domain waveform jumps from positive to negative during the merger-ringdown. This the most valid interpretation for this scenario is that of the direction of the spin, $j(t)\to j_f$, evolving drastically during this regime, in particular, going from positive to negative. It seems that one should **not** interpret the two frequencies in this case as being simply a superposition of $m>0$ and $m<0$ as the transition between spin orientations is not trivially the transition in dominance between one QNM and the other. The related question is ***What does the spin evolution look like for these cases?*** Upon further thought, there appear to be two core scenarios:

(S1) The direction of $\hat{j}(t)$ inverts during the system's evolution, leaving the final perturbation to be dominantly prograde relative to $\hat{j}_f = -\hat{j}_i$.

(S2) The direction of $\hat{j}(t)$ stays "fixed" throughout the system's evolution, but the perturbation transitions from prograde to be dominantly retrograde relative to $\hat{j}_f$.

f. To-Do List: —

- Add plot of QNM frequency fit points on 2D colormap of `leaver_workfunction` at fixed separation constant to further illustrate.
- **Implement as full waveform model in python before continuing!**
  - Make polynomial model for separation constants.
  - Were/Are phases of frequencies and separation constants consistent for spheroidal harmonic calculation?
- The model has been changed so that the overall eta dependence is not dependent on the overtone number.
- Recent work in analytic perturbation theory suggests, if I recall correctly, that the overtones may be a guage artifact. **Is this a correct statement and does it apply here?**
- There seems to be a problem with the current $(2,1,0)$ QNM frequency: when using the imaginary part for $\mathcal{K}_k^{\text{c}}$ fitting, the nearly extremal Kerr behavior (*i.e.* it derivatives) seems to be inconsistent with the numerical data.

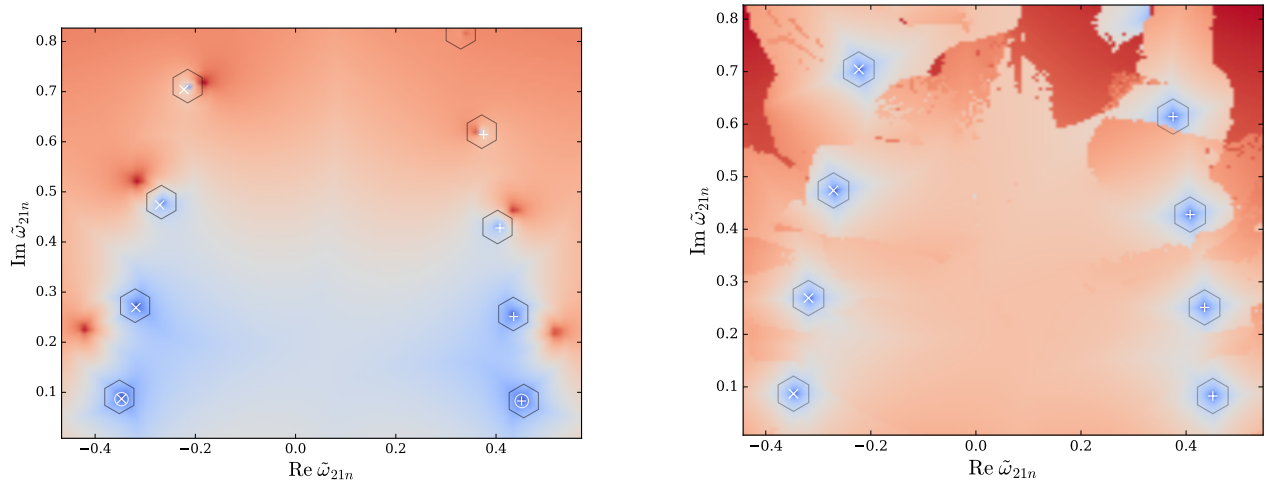

FIG. 1. Fits on leaver solutions

Appendix A: A Complex Polynomial Model for Dimensionless QNM Frequencies

While it is possible to refer to the work of Leaver and others to numerically compute the QNM frequencies of Kerr, it is more convenient to utilize a closed form function, in particular, a fit to the numerical values, for the same task. This section details such a fit for the dimensionless QNM frequency, $\tilde{\Omega}_k$ (See Equation 4), as well as brief comparisons with similar fits in the literature. Previous fits separately model the real and imaginary parts of $\tilde{\Omega}_k$ on $0 \leq j_f < 1$, and treat prograde and retrograde QNM disjointly [3]. Here we recognize that the retrograde frequencies may be associated with negative black hole spin (*e.g.* one pointing oppositely of an initial orbital angular momentum direction). This point illuminates that the prograde and retrograde QNM frequencies are continuously connected as j_f transitions from positive to negative. We therefore construct a model, $\tilde{\Omega}_k(j_f)$, where the domain, j_f, ranges from -1 to 1.

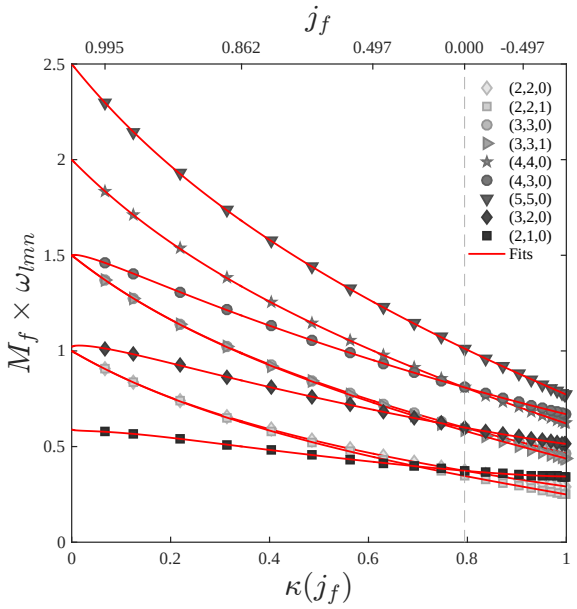

FIG. 2. Fits of dimensionless QNM central frequencies (solid lines) along with select numerical values (grey markers) computed using Leaver's method [4]. Before the application of $\kappa(j_f)$, points are spaced between -0.995 and 0.995 according to 0.995 times the sin of a fiducial angle which is uniformly spaced between $-\pi/2$ and $\pi/2$. Values of j_f are shown in the upper axis for κ at $l = m$. The grey dashed line marks the value of κ where $j_f = 0$.

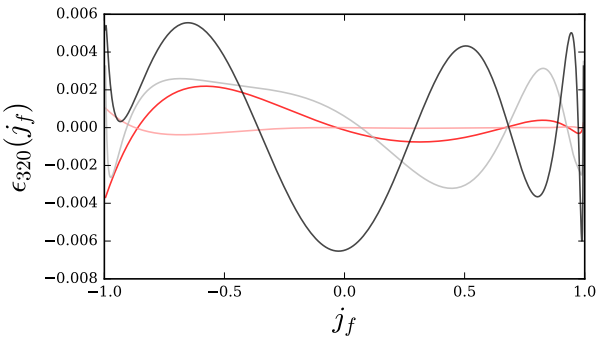

FIG. 3. Residuals of Leaver's constraint equations for QNM solutions to Teukolsky's equations. The equations are ... the quantities are ...

Furthermore, noting that each QNM frequency, $\tilde{\Omega}_k$, changes rapidly near $j_f \approx 1$, we chose to perform a domain mapping, $\kappa(j_f)$, prior to fitting. We find that defining $\kappa(j_f)$ as

$$\kappa(j_f) = \left(\log_3[2 - j_f]\right)^{1/(|s|-|m|+l)} \quad (s = -2)\,. \tag{A1}$$

effectively maps $(-1, 1)$ to $(1, 0)$ while simultaneously simplifying the behavior of each $\tilde{\Omega}_k$ near $j_f = 1$. This simplification corresponds to the largely linear and parabolic behavior of the QNM frequencies shown in Figure (2).

After applying Equation (A1) to j_f, we find that all of the QNM frequencies considered here are extremely well modeled by a polynomial of order 4 whose coefficients are complex (See Equations B2-B10). Information from the near-

extremal Kerr perturbation theory has been utilized (*e.g.* [5–8]). In particular, Equations (B2-B10) have been constructed to be consistent with the zero damped mode (ZDM) branch of the nearly extremal Kerr limit where, as $j_f \to 0$, the real part of the complex QNM frequency tends to $m/2$, the critical frequency for super-radiance. Therefore the fitting formula take on the generalized form

$$\tilde{\Omega}_{lmn}(\kappa) \;=\; m/2 \;+\; \sum_p g_p\, \kappa^p \;, \tag{A2}$$

where g_p are complex valued. This fitting ansatz aims to reproduce the ZDM branch of the Kerr spectrum. The damped-mode branch of the nearly extremal Kerr spectrum is not treated in the fit.

$$\tilde{\Omega}_{220}(\kappa) \;=\; 1.0 \;+\; \kappa\,(1.5578e^{2.9031i} \;+\; 1.9510e^{5.9210i}\kappa \;+\; 2.0997e^{2.7606i}\kappa^2 \;+\; 1.4109e^{5.9143i}\kappa^3 \;+\; 0.4106e^{2.7952i}\kappa^4\,) \tag{A3}$$

$$\tilde{\Omega}_{221}(\kappa) \;=\; 1.0 \;+\; \kappa\,(1.8709e^{2.5112i} \;+\; 2.7192e^{5.4250i}\kappa \;+\; 3.0565e^{2.2857i}\kappa^2 \;+\; 2.0531e^{5.4862i}\kappa^3 \;+\; 0.5955e^{2.4225i}\kappa^4\,) \tag{A4}$$

$$\tilde{\Omega}_{330}(\kappa) \;=\; 1.5 \;+\; \kappa\,(2.0957e^{2.9650i} \;+\; 2.4696e^{5.9967i}\kappa \;+\; 2.6655e^{2.8176i}\kappa^2 \;+\; 1.7584e^{5.9327i}\kappa^3 \;+\; 0.4991e^{2.7817i}\kappa^4\,) \tag{A5}$$

$$\tilde{\Omega}_{331}(\kappa) \;=\; 1.5 \;+\; \kappa\,(2.3391e^{2.6497i} \;+\; 3.1399e^{5.5525i}\kappa \;+\; 3.5916e^{2.3472i}\kappa^2 \;+\; 2.4490e^{5.4435i}\kappa^3 \;+\; 0.7004e^{2.2830i}\kappa^4\,) \tag{A6}$$

$$\tilde{\Omega}_{440}(\kappa) \;=\; 2.0 \;+\; \kappa\,(2.6589e^{3.0028i} \;+\; 2.9783e^{6.0510i}\kappa \;+\; 3.2184e^{2.8775i}\kappa^2 \;+\; 2.1276e^{5.9897i}\kappa^3 \;+\; 0.6034e^{2.8300i}\kappa^4\,) \tag{A7}$$

$$\tilde{\Omega}_{430}(\kappa) \;=\; 1.5 \;+\; \kappa\,(0.2050e^{0.5953i} \;+\; 3.1033e^{3.0162i}\kappa \;+\; 4.2361e^{6.0388i}\kappa^2 \;+\; 3.0289e^{2.8262i}\kappa^3 \;+\; 0.9084e^{5.9152i}\kappa^4\,) \tag{A8}$$

$$\tilde{\Omega}_{550}(\kappa) \;=\; 2.5 \;+\; \kappa\,(3.2405e^{3.0279i} \;+\; 3.4906e^{6.0888i}\kappa \;+\; 3.7470e^{2.9212i}\kappa^2 \;+\; 2.4725e^{6.0365i}\kappa^3 \;+\; 0.6994e^{2.8766i}\kappa^4\,) \tag{A9}$$

$$\tilde{\Omega}_{320}(\kappa) \;=\; 1.0225e^{0.0049i} \;+\; 0.2473e^{0.6653i}\kappa \;+\; 1.7047e^{3.1383i}\kappa^2 \;+\; 0.9460e^{0.1632i}\kappa^3 \;+\; 1.5319e^{5.7036i}\kappa^4 \;+\; 2.2805e^{2.6852i}\kappa^5 \;+\; 0.9215e^{5.8417i}\kappa^6 \tag{A10}$$

$$\tilde{\Omega}_{210}(\kappa) \;=\; 0.5891e^{0.0435i} \;+\; 0.1890e^{2.2899i}\kappa \;+\; 1.1501e^{5.8101i}\kappa^2 \;+\; 6.0459e^{2.7420i}\kappa^3 \;+\; 11.1263e^{5.8441i}\kappa^4 \;+\; 9.3471e^{2.6694i}\kappa^5 \;+\; 3.0384e^{5.7915i}\kappa^6 \tag{A11}$$

Figure (2) shows the fits and related numerical data for all QNMs considered here. Figure (3) shows the related (percentage) residual errors over the calibration region, with

$$\%\Delta\omega_k \;=\; \%\Delta M_f\omega_k \;=\; 100\times(\omega_k^{\rm Fit}-\omega_k)/|\omega_k| \tag{A12}$$

and

$$\%\Delta(1/\tau_k) \;=\; \%\Delta(M_f/\tau_k) \;=\; 100\times(1/\tau_k^{\rm Fit}-1/\tau_k)/(1/\tau_k)\;. \tag{A13}$$

While 61 calibration points were used for the fit, only 21 points are shown for clarity. As the model encapsulated by Equations (B2-B10) has only been calibrated for j_f on $(-0.995, 0.995)$, nearly extremal spin features of the QNM frequencies, such as zero damping branching (*e.g* [8]), are *not* captured by the model presented here.

The model presented in this section applies to the $-m$ QNMs according to

$$\tilde{\Omega}^*_{lmn} \;=\; -\tilde{\Omega}^*_{lm'n}, \text{ where } m' \;=\; -m\;, \tag{A14}$$

and $*$ denotes complex conjugation.

Moreover, it is also of practical use to note that one may trivially obtain dimentionful QNM frequencies by scaling by the black hole mass:

$$\tilde{\omega}_k \;=\; \tilde{\Omega}_k/M_f\;.$$

In practice, $\tilde{\omega}_k$ (*i.e.* $\tilde{\omega}_{lmn}$) are most often used (*e.g.* as in Equation 2).

Appendix B: A Complex Polynomial Model for QNM Separation Constants

The QNM separation constants are needed in order to compute the spheroidal harmonic functions according to [Add Equation]. Here, we use the same domain mapping as in Section (A). In addition we consider the complex valued separation constant's real and imaginary parts separately

$$\mathcal{K}_k \;=\; \mathcal{K}_k^{\rm r} \;+\; i\,\mathcal{K}_k^{\rm c}\;. \tag{B1}$$

For $\mathcal{K}_k^{\rm r}$, a direct polynomial fit is applied. For $\mathcal{K}_k^{\rm c}$, where there are natural roots (e.g. at $j_f = 0$, and in the case of the modes with zero damping as $j_f \to 1$, $j_f = 1$), we scale away the simplest polynomial form associated with these roots before fitting, and rescale afterwards. This has the effect of simplifying the fit and enforcing strict root locations. Although performed separately, the two fits are combined according to Equation (B1). The resulting fit equations are by Equations (B2-B10). Note that the number of significant digits shown here is limited for brevity. Fitting parameters at full precision may be found on github.

$$\mathcal{K}_{220}(\kappa) = 0.5526e^{0.0000i} + 6.5427e^{0.2444i}\kappa + 5.9466e^{3.8841i}\kappa^2 + 5.3930e^{1.0165i}\kappa^3 + 3.5870e^{4.5340i}\kappa^4 + 1.3686e^{1.5708i}\kappa^5 + 0.1852e^{4.7124i}\kappa^6 \quad \text{(B2)}$$

$$\mathcal{K}_{221}(\kappa) = 0.5523e^{0.0000i} + 7.9407e^{0.6408i}\kappa + 12.5557e^{4.4198i}\kappa^2 + 13.6852e^{1.4804i}\kappa^3 + 10.4388e^{4.7260i}\kappa^4 + 4.2073e^{1.5708i}\kappa^5 + 0.7623e^{4.7124i}\kappa^6 \quad \text{(B3)}$$

$$\mathcal{K}_{210}(\kappa) = 3.1009e^{6.2582i} + 2.6921e^{1.9585i}\kappa + 16.5858e^{4.9842i}\kappa^2 + 57.8409e^{1.6372i}\kappa^3 + 118.2176e^{4.7267i}\kappa^4 + 135.9399e^{1.5708i}\kappa^5 + 82.8174e^{4.7124i}\kappa^6 + 20.8517e^{1.5708i}\kappa^7 \quad \text{(B4)}$$

$$\mathcal{K}_{330}(\kappa) = 5.7047e^{0.0000i} + 7.9443e^{0.1804i}\kappa + 6.5510e^{3.7793i}\kappa^2 + 6.3142e^{0.9386i}\kappa^3 + 4.8121e^{4.4691i}\kappa^4 + 2.3893e^{1.5708i}\kappa^5 + 0.4808e^{4.7124i}\kappa^6 \quad \text{(B5)}$$

$$\mathcal{K}_{331}(\kappa) = 5.7032e^{0.0000i} + 8.9493e^{0.4983i}\kappa + 12.7053e^{4.3177i}\kappa^2 + 15.6353e^{1.3939i}\kappa^3 + 14.1906e^{4.6691i}\kappa^4 + 7.3324e^{1.5708i}\kappa^5 + 1.5370e^{4.7124i}\kappa^6 \quad \text{(B6)}$$

$$\mathcal{K}_{320}(\kappa) = 8.1854e^{6.2760i} + 1.5519e^{1.7909i}\kappa + 8.9465e^{5.1868i}\kappa^2 + 28.6605e^{1.6366i}\kappa^3 + 60.7779e^{4.7211i}\kappa^4 + 72.1324e^{1.5708i}\kappa^5 + 45.3812e^{4.7124i}\kappa^6 + 11.8471e^{1.5708i}\kappa^7 \quad \text{(B7)}$$

$$\mathcal{K}_{440}(\kappa) = 13.0529e^{0.0000i} + 9.2346e^{0.1418i}\kappa + 7.0905e^{3.6918i}\kappa^2 + 6.4671e^{0.8925i}\kappa^3 + 4.9691e^{4.4385i}\kappa^4 + 2.6230e^{1.5708i}\kappa^5 + 0.5817e^{4.7124i}\kappa^6 \quad \text{(B8)}$$

$$\mathcal{K}_{430}(\kappa) = 15.2887e^{0.0000i} + 0.7530e^{0.2205i}\kappa + 3.6494e^{0.6164i}\kappa^2 + 8.0253e^{4.8276i}\kappa^3 + 12.4721e^{1.6733i}\kappa^4 + 10.3028e^{4.7124i}\kappa^5 + 3.5289e^{1.5708i}\kappa^6 \quad \text{(B9)}$$

$$\mathcal{K}_{550}(\kappa) = 22.5229e^{0.0000i} + 10.4414e^{0.1161i}\kappa + 7.7971e^{3.6125i}\kappa^2 + 6.5999e^{0.8379i}\kappa^3 + 4.9037e^{4.4055i}\kappa^4 + 2.5991e^{1.5708i}\kappa^5 + 0.5899e^{4.7124i}\kappa^6 \quad \text{(B10)}$$

Appendix C: A Model for the Spheroidal Harmonic Normalization Constants

It is useful to be able to normalize the spheroidal harmonic functions. While the normailzation constants reduce to those of the spin -2 spherical harmonics for $j_f = 0$, an analytic form for all spins is not known at the time of this publication. Therefore, we present a polynomial fit for the normalization constants for the QNM used here.

The spheroidal harmonic functions, $\mathcal{S}_k(j_f M_f \tilde{\omega}_k, \theta, \phi)$, were calculated according to Leaver's solution with no additional scaling [4]. We define the normalization constant, C_k, such that

$$\int_\Omega \mathcal{S}_k^* \mathcal{S}_k \, d\Omega = 1 \quad \text{(C1)}$$

We find that the resulting normalization constants are well captured, with all residual errors less than 0.5%, by Equations (C2-C10).

$$C_{220}(\kappa) = 7.8637 - 3.6145\kappa + 3.4900\kappa^2 - 2.2935\kappa^3 + 0.7443\kappa^4 \quad \text{(C2)}$$

$$C_{221}(\kappa) = 7.8630 - 3.5987\kappa + 2.8846\kappa^2 - 0.9274\kappa^3 - 0.0445\kappa^4 \quad \text{(C3)}$$

$$C_{330}(\kappa) = 3.5163 + 0.1650\kappa + 1.3011\kappa^2 - 0.8362\kappa^3 + 0.8202\kappa^4 \quad \text{(C4)}$$

$$C_{331}(\kappa) = 3.5153 + 0.1929\kappa + 0.9681\kappa^2 - 0.0055\kappa^3 + 0.2498\kappa^4 \quad \text{(C5)}$$

$$C_{440}(\kappa) = 1.7539 + 1.0011\kappa + 1.5550\kappa^2 - 1.2234\kappa^3 + 1.6462\kappa^4 \quad \text{(C6)}$$

$$C_{550}(\kappa) = 0.9135 + 0.8957\kappa + 2.5440\kappa^2 - 2.8244\kappa^3 + 3.2814\kappa^4 \quad \text{(C7)}$$

$$C_{210}(\kappa) = 3.0439 - 0.0688\kappa + 0.8767\kappa^2 - 3.9221\kappa^3 + 8.5963\kappa^4 - 8.5220\kappa^5 + 3.3115\kappa^6 \quad \text{(C8)}$$

$$C_{320}(\kappa) = 0.7485 - 0.0816\kappa + 1.0375\kappa^2 - 3.2793\kappa^3 + 7.2458\kappa^4 - 7.4132\kappa^5 + 3.0606\kappa^6 \quad \text{(C9)}$$

$$C_{430}(\kappa) = 0.3954 - 0.0992\kappa + 1.5285\kappa^2 - 5.0993\kappa^3 + 10.9565\kappa^4 - 10.9991\kappa^5 + 4.5221\kappa^6 \quad \text{(C10)}$$

[1] L. London, D. Shoemaker, and J. Healy, "Modeling ringdown: Beyond the fundamental quasinormal modes," *Phys. Rev.*, vol. D90, no. 12, p. 124032, 2014.

[2] W. G. Anderson, P. R. Brady, J. D. E. Creighton, and E. E. Flanagan, "An Excess power statistic for detection of burst sources of gravitational radiation," *Phys. Rev.*, vol. D63, p. 042003, 2001.

[3] E. Berti, V. Cardoso, and C. M. Will, "On gravitational-wave spectroscopy of massive black holes with the space interferometer LISA," *Phys. Rev.*, vol. D73, p. 064030, 2006.

[4] E. Leaver, "An Analytic representation for the quasi normal modes of Kerr black holes," *Proc.Roy.Soc.Lond.*, vol. A402, pp. 285–298, 1985.

[5] O. J. C. Dias, M. Godazgar, and J. E. Santos, "Linear Mode Stability of the Kerr-Newman Black Hole and Its Quasinormal Modes," *Phys. Rev. Lett.*, vol. 114, no. 15, p. 151101, 2015.

[6] A. Zimmerman, H. Yang, F. Zhang, D. A. Nichols, E. Berti, and Y. Chen, "Reply to "On the branching of quasinormal resonances of near-extremal Kerr black holes" by Shahar Hod," 2015.

[7] A. Zimmerman and Z. Mark, "Damped and zero-damped quasinormal modes of charged, nearly extremal black holes," *Phys. Rev.*, vol. D93, no. 4, p. 044033, 2016. [Erratum: Phys. Rev.D93,no.8,089905(2016)].

[8] H. Yang, F. Zhang, A. Zimmerman, D. A. Nichols, E. Berti, and Y. Chen, "Branching of quasinormal modes for nearly extremal Kerr black holes," *Phys. Rev.*, vol. D87, no. 4, p. 041502, 2013.